

---

V.I. MARENKOV

I.I. Mechnikov Odessa National University  
(2, Dvoryanska Str., Odessa 65026, Ukraine; e-mail: maren0@ukr.net)

**RADIATION EMISSION  
BY NANOPARTICLES IN HETEROGENEOUS  
PLASMA WITH A CONDENSED DISPERSED PHASE**

---

PACS 52.25.-b, 52.90.+z,  
52.70.Gw

*In the framework of the statistical “cell” approach to the description of the ionization in heterogeneous plasma (HP), the mechanism of braking radiation generation in the bulk of heterogeneous plasma formations has been studied. A new model was proposed for the description of the effective interaction between microfields and charges in plasma. The stochastic motion of charged particles in HP is considered as an evolution of anharmonic oscillations executed by separate charges in an instant field of electric forces in the electroneutral cell. The effective values of frequency and the specific integral power of the braking radiation from HP in the radio-frequency spectral range are calculated by averaging over the ensemble of cells. The amplitude-frequency function and the relative contributions of separate oscillation modes of plasma charges to the emitted radiation intensity are determined in the framework of the random phase approximation. A comparative analysis of the data obtained in the model theory and the experimental ones obtained for plasma with aluminum oxide nanoparticles was carried out in the space of key HP parameters. A good agreement was obtained between the results of computer-assisted simulation and the experimental data both at the qualitative and quantitative levels. Possibilities to apply the results obtained for making telediagnosics of heterogeneous plasma formations were discussed.*

*Keywords:* cell, quasi-neutrality, heterogeneous plasma formation (HPF), heterogeneous plasma, condensed dispersed phase (CDPh), braking radio-frequency radiation of the plasma, telediagnosics.

## 1. Introduction

High-temperature emissions of industrial aerosols, ionized dusty gas formations in the atmosphere and in space, decay products of meteorites at their interaction with the Earth atmosphere, aggregates of space dust under the conditions of ionizing radiation, products of surface ablation in high-velocity and high-temperature gas flows – this is a list of objects of the terrestrial and space origins – this list is far from being complete – for which ionization of structural units (dust macroparticles and gas atoms and molecules) is sufficient for the quasi-neutrality in the volume to be

established owing to long-range electromagnetic interactions between particles [1–8]. In other words, such objects in view of their high specific energy contributions and, as a consequence, a substantial resulting ionization of structural elements acquire plasma properties. In this case, the role of energy suppliers for separate system components is usually played by external (ionizing radiation) or internal (exothermic plasma-chemical reactions) ionization sources [1–5]. The majority of such processes are nonequilibrium. They are accompanied by the presence of macroscopic energy, momentum, mass, and electric charge flows in the volume of heterogeneous plasma formation (HPF) itself [6].

At the same time, the lightest in the HPF is the electron subsystem. It is characterized by a relaxation time that is shorter by many orders of magnitude than all other time scales of relaxation processes directed at establishing the local thermodynamic equilibrium (LTE) in the system. The electron subsystem quickly “traces” changes in the local self-consistent electrostatic field in the LTE regions of a plasma system. The consideration of electron-ion processes in HPFs based on the model of quasi-neutral plasma cells and carried out in the framework of the “adiabatic approximation analog” opens new capabilities for the research and description of braking radiation emission in the LTE regions of nonequilibrium plasma systems [6–10]. In particular, monitoring the evolution of braking radiation and the intensity of its “particle” component in the signal emitted by heterogeneous plasma with a condensed dispersed phase (CDP), it is possible to study the parameters of the relevant heavy subsystem, i.e. an ensemble of CDP particles. Specific contributions of anharmonic oscillations executed by separate charges govern the intensity and the profile of the amplitude-frequency function for the braking radiation emitted by HPFs. A comparative analysis of relative intensities inherent to the spectral components of HPF radio signals carried out in the framework of the inverse problem of the “statistical cell approach” provides the access to information concerning the electrophysical parameters of the gaseous and condensed dispersed phases. In a vast number of monographic publications (see, e.g., works [11–16]) and separate papers, the braking radiation emission by macroparticles in thermal plasma has not obtained enough attention, both in the experimental and theoretical aspects. The statistical issues faced with when theoretically describing electron-ion braking radiation processes in heterogeneous plasma comprise the main goal of researches in this work.

## 2. Local Electrostatic Field of Plasmosol

In the model of statistical electroneutral cells for a rarefied plasmosol (a system of emitting macroparticles, buffer gas, and electrons [5–10]), the distribution of a self-consistent electrostatic potential  $\varphi(r)$  in the free cell volume,  $C'_\xi = C_\xi - V_p$ , is described by the Poisson–Boltzmann equation, and the solution of the

latter is expressed by the formula

$$\varphi(r) = \frac{\alpha}{\kappa r} \left\{ \kappa r r_C \operatorname{ch}[\kappa(r_C - r)] - \operatorname{sh}[\kappa(r_C - r)] - \kappa r \right\}, \quad (2.1)$$

where  $r$  is the radial coordinate,  $r_C$  the radius of spherical electroneutral cell,  $\kappa = \sqrt{\frac{4\pi e^2}{kT} n_{e0}}$  is the reciprocal Debye length of free electrons in the HPF,  $k$  is the Boltzmann constant,  $e$  the elementary charge,  $T$  the absolute temperature,  $n_{e0}$  the concentration of electrons at the cell boundary, and  $\alpha = \frac{kT}{e}$  is the problem parameter. Within the own volume of a selected macroparticle,  $\mathbf{r} \in V_p$ , the self-consistent electrostatic potential  $\tilde{\varphi}(r)$  satisfies the Poisson–Fermi equation

$$\frac{d^2 \tilde{\varphi}}{dr^2} + \frac{1}{r} \frac{d\tilde{\varphi}}{dr} = -\frac{4e}{3\pi \varepsilon_p} \times \left( \frac{2m_e}{\hbar^2} \right)^{3/2} \left[ (E_F^0)^{3/2} - (E_F)^{3/2} \right]. \quad (2.2)$$

Here,  $\varepsilon_p$  is the relative dielectric permittivity of the macroparticle substance,  $m$  the electron mass,  $\hbar = \frac{h}{2\pi}$  is the Dirac constant,  $E_F^0$  is the Fermi energy of conduction electrons in the nonperturbed macroparticle substance, and  $E_F = E_F(r)$  is the local Fermi energy value.

The solution of Eq. (2.2) determines the distribution of the self-consistent electrostatic potential in the macroparticle body reckoned from its value at the body center. This value, which is selected as the potential zero, differs by the constant  $C$  from the zero point of “external” potential at the cell boundary. Therefore, the constant  $C$  must be determined from the matching condition for the “external” and “internal” potentials across the macroparticle boundary, i.e. at  $r = r_p$ ,

$$\tilde{\varphi}(r_p) = \varphi(r_p) + C. \quad (2.3)$$

Another condition, which makes the problem “closed”, is the continuity of the normal component of the electrostatic induction  $\mathbf{D} = \varepsilon \mathbf{E}$  at the macroparticle surface; it looks like

$$\varepsilon_p \left. \frac{\partial \tilde{\varphi}}{\partial r} \right|_{r=r_p} = \varepsilon_G \left. \frac{\partial \varphi}{\partial r} \right|_{r=r_p}. \quad (2.4)$$

Making allowance for Eqs. (2.3) and (2.4), the function  $\tilde{\varphi}(r)$  is determined in the form

$$\tilde{\varphi}(r) = \tilde{\alpha} \cdot [\operatorname{sh}(\kappa_F r) / \kappa_F r - 1]. \quad (2.5)$$

The reciprocal Fermi length of conduction electrons,  $\tilde{\kappa}_F$ , and the parameter  $\tilde{\alpha}$  in Eq. (2.5) are given by the following formulas:

$$\kappa_F = \left[ \frac{2e^2}{\pi\epsilon_p} \left( \frac{2m_e}{\hbar^2} \right)^{3/2} \sqrt{E_F^0(1 + \tilde{F} - \tilde{F}^0)^{1/2}} \right]^{1/2}, \quad (2.6)$$

$$\tilde{\alpha} = \frac{2}{3} \frac{E_F^0}{e} \left[ (1 + \tilde{F} - \tilde{F}^0) - (1 + \tilde{F} - \tilde{F}^0)^{-1/2} \right]. \quad (2.7)$$

Solutions (2.1) and (2.5) for the Poisson–Boltzmann and Poisson–Fermi equations were obtained with the use of the Neumann–Dirichlet boundary conditions and in the linear approximation in the corresponding potential, namely, the potential at the boundaries of free cell volume for the “external” potential,  $\varphi(r)$ , and the potential in the own macroparticle volume for the “internal” one,  $\tilde{\varphi}(r)$ . The homogeneous Neumann conditions were imposed at the  $C_\xi^z$ -cell boundary for the external problem (because the cell is electrically neutral as a whole) and at the macroparticle center for the internal one (bearing in mind the symmetry of potential distribution). The matching of the found solutions across the macroparticle surface brings us ultimately to the final equation for the Fermi level of the HPF electron component in the LTE regions of plasma,

$$\begin{aligned} \Omega(F) = & \frac{\tilde{\alpha}\epsilon_p\kappa E_F^0}{\tilde{\kappa}_F kT} \frac{\text{ch}(\tilde{\kappa}_F r_p)}{\text{ch}[\kappa(r_C - r_p)]} \times \\ & \times [\tilde{\kappa}_F r_p - \text{th}(\tilde{\kappa}_F r)] - \kappa(r_C - r_p) + \\ & + (1 - \kappa^2 r_C r_p) \text{th}[\kappa(r_C - r_p)] = 0. \end{aligned} \quad (2.8)$$

The electron characteristics of HPF were determined with the use of solutions (2.1), (2.5), and (2.8) in a computer-assisted experiment for a given set of key parameters, such as the temperature, the concentration and the size of macroparticles, and the dielectric and electronic characteristics of a macroparticle substance. In Table 1, the values obtained for the Fermi level, the macroparticle charge, the electron concentration in the HPF, and the surface potential of  $\text{Al}_2\text{O}_3$  particles normalized by the thermal energy,  $\Phi_p^e \equiv \Phi^e(r_p) = \frac{e\varphi_p}{kT}$ , are quoted. They were calculated for the temperatures that are characteristic of plasma obtained as a combustion product of aluminum-based rocket fuels [17–19]. The charge  $z$  is expressed in elementary charge units, and the dimensionality of the calculated electron concentration is  $[n_{e0}] = \text{cm}^{-3}$ .

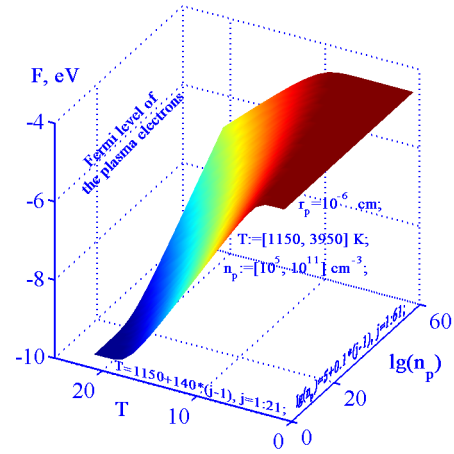


**Fig. 1.** Dependence of the Fermi level for the electron component in the HPF on the concentration of CDP particles and the temperature  $T$  in a locally equilibrium volume of plasma

The local ionization parameters of HPF are unequivocal functions of the Fermi level of free electrons at the concentration  $n_{e0}$ . Therefore, the functions  $F = F(T, n_p, r_p, \epsilon_p W^0, E_c^0)$ , which are similar to that depicted in Fig. 1, were determined in the numerical experiment and directly used in the calculations of HPF parameters, namely, the intensities of the spectral components of braking radiation emitted by macroparticles and electrons. The statistical model of anharmonic oscillation processes in the subsystem of HPF charges is considered in the next section.

### 3. Anharmonic Oscillation Motion of Charges

A fluctuation-induced or externally activated shift of a separate charge in an effective electroneutral HPF

**Table 1.** HPF parameters at various temperatures

No.	$T$ , K	$F$ , eV	$z$	$\lg(n_{e0})$
0	2750	−6.8807	1.7109	8.2331
1	2830	−7.0662	1.8967	8.2779
2	2910	−7.2516	2.0938	8.3208
3	2990	−7.4368	2.3045	8.3624
4	3070	−7.6214	2.5313	8.4032
5	3150	−7.8053	2.7777	8.4435
6	3230	−7.9881	3.0484	8.4839
7	3310	−8.1695	3.3497	8.5248
8	3390	−8.3492	3.6904	8.5669
9	3470	−8.5264	4.0834	8.6108
10	3550	−8.7005	4.5477	8.6576

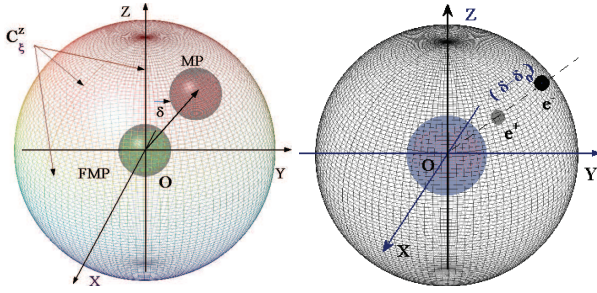


Fig. 2

cell (Fig. 2) is equivalent to a chain of consecutive stages in an anharmonic oscillation motion of the shifted charge in a perturbed electrostatic field of an averaged cell  $C_\xi^z$  that relaxes to the equilibrium state. In Figs. 2, a and 2, b, the cells  $C_\xi^z$  perturbed by the shift of a macroparticle or an electron, respectively, are shown. The shift of a macroparticle is always reckoned from the origin of Lagrange coordinates, and that of an electron from its initial position.

Every position  $\delta$  with respect to the center of the shifted charge cell is characterized by a certain quasi-elastic coefficient  $\mu$  of the perturbed cell, which is determined by an instant value of the force  $\mathbf{f} = \mathbf{f}(\delta)$  acting upon the charge. Therefore, every particle shifted from its equilibrium position executes a complicated oscillation motion in the cell. At every moment, this motion around the point of instant particle localization can be characterized by a certain cyclic frequency, which would be inherent to particle oscillations within the time interval  $[0, \tau]$ , where  $\tau$  is the relaxation time, provided that the quasi-elastic coefficient of the cell remained constant in the course of relaxation.

The model of anharmonic oscillation motion for a separate macroparticle is based on two basic assumptions:

1. The average macroparticle charge obtained by statistically averaging it over the ensemble of instant cells coincides with the value obtained by averaging the charge over the Gibbs ensemble.

2. The distribution of the self-consistent electrostatic field in a cell perturbed by a shifted charge (a macroparticle or an electron) is governed by a combined action of the nonperturbed cell field and an effective dipole formed by the shifted macroparticle and a fictitious macroparticle (FMP). The charge distribution on the latter is identical to that on the real

particle, but has an opposite polarity (as shown in Fig. 2, a). The FMP is always located at the origin of coordinates.

According to Heisenberg's uncertainty principle, the shifts of electrons from their equilibrium positions and their localization in space at temperatures  $T \sim 2000$  K cannot be determined with an accuracy better than  $\Delta\delta \sim 10^{-8}$  cm. This restriction "from below" on the average determination accuracy of the electron position in space confines the upper frequency limit for the braking radiation emitted by the electron component in thermal plasma.

For short enough time intervals, the shift of a charged particle  $|\varsigma| = |\delta - \delta_0| \ll 1$ , and the equation of its anharmonic oscillatory motion can be written down as follows:

$$m_j \ddot{\delta} = -\mu \varsigma. \quad (3.1)$$

The subscript  $j$  marks the kind of a shifted particle:  $j = p$  for the macroparticle and  $j = e$  for the electron. The quasi-elastic coefficient  $\mu$  for a cell at every moment is a tensor, but only its radial component survives at the statistical averaging, so that Eq. (3.1) takes the scalar form

$$m_j \ddot{\delta} = -\frac{f_j(\delta) |(\delta - \delta_0)|}{((\delta - \delta_0)\delta)}. \quad (3.2)$$

The radial component of the force in Eq. (3.2) can be determined from the following reasoning. Let an FMP be put at the cell center, with the charge distribution on the FMP being identical to that on the central macroparticle, but its polarity having the opposite sign with respect to the charge of a selected macroparticle. Then, the average field created in the cell volume by all charges in the system, except the central one (the neutralized FMP), is not changed. As follows from the principle of field superposition in electrodynamics [9], the actual field strength in the volume  $C_\xi^z$  is determined by the vector sum of the field created by the charge environment of a central macroparticle and the field of its own charge. If the central charge becomes shifted, the resulting field in the cell changes by the combined contribution from the "fictitious charge" and macroparticle fields. This consideration is an analog of the application of the electrostatic specular reflection method in order to determine the average field in a cell perturbed by the shift of a central macroparticle (see

Fig. 2). This enables us to obtain, in the dipole approximation, the magnitude of central electrostatic force that acts on a separate shifted charge in the electroneutral cell perturbed by this shift  $\varsigma$ . Note that the effective dipole “macroparticle–FMP” determines here only one force component. Therefore, the instant frequency of anharmonic macroparticle oscillations, in this sense, is not the frequency of a dipole vibrator, because the coefficient of cell quasi-elasticity (see Eq. (3.1)) depends, first of all, on the distribution of the self-consistent electrostatic potential gradient in a nonperturbed cell, being only partially modified by the dipole contribution of the interaction between the particle and its image. As is seen from Eqs. (3.1) and (3.2), the cyclic frequency of the particle in the field of a quasi-elastic force arising in the perturbed cell equals

$$\omega = \left( \sqrt{\frac{\mu}{m_j}} \right). \quad (3.3)$$

On the basis of formulas presented in Section 2, the forces acting on macroparticles and electrons located in HPF cells can be expressed as functions of their (macroparticles and electrons) initial,  $\delta_0$ , and current,  $\delta$ , positions as follows:

$$\begin{aligned} f_p(\delta) &= -ze \left. \frac{d\varphi}{dr} \right|_{r=\delta} - \frac{z^2 e^2}{\delta^2} = \frac{\alpha^2}{\kappa^2 \delta^2} \times \\ &\times \{ \kappa(r_C - \delta) \text{ch}[\kappa(r_C - \delta)] - \\ &- (1 - \kappa^2 r_C \delta) \text{sh}[\kappa(r_C - \delta)] \} \times \\ &\times \left\{ x \text{ch}(x) - (1 - x^2 r_C r_p) \text{sh}x \right\} - \frac{z^2 e^2}{\delta^2}; \end{aligned} \quad (3.4)$$

$$\begin{aligned} f_e(\delta) &= +e \left. \frac{d\varphi}{dr} \right|_{r=\delta} - \frac{e^2 \text{Sign}(\delta - \delta_0)}{(\delta - \delta_0)^2} = \\ &= \frac{\alpha e}{\kappa \delta^2} \left\{ \kappa(r_C - \delta) \text{ch}[\kappa(r_C - \delta)] - \right. \\ &\left. - (1 - \kappa^2 r_C \delta) \text{sh}[\kappa(r_C - \delta)] \right\} - \frac{e^2 \text{Sign}(\delta - \delta_0)}{(\delta - \delta_0)^2}. \end{aligned} \quad (3.5)$$

To make the formulas more compact, we will use below the notations  $\{\cdot\delta\cdot\}$  and  $\{\cdot r_p \cdot\}$  for the expressions in the braces of formulas (3.4) and (3.5), which contain or do not contain, respectively, the quantity  $\delta$ . Then, for instance, the equation of anharmonic oscillations (3.2) for the macroparticle (see Eq. (3.4)) takes the form

$$m_p \ddot{\delta} = \frac{z^2 e^2}{\delta^2} \left[ \frac{\{\cdot\delta\cdot\}}{\{\cdot r_p \cdot\}} - 1 \right]. \quad (3.6)$$

and the quasi-elastic coefficient  $\mu_p$  for the perturbed cell  $C_\xi^z$  and the frequency of quasi-elastic macroparticle oscillations, both considered as functions of the particle shift, satisfy the relations

$$\mu_p = \frac{z^2 e^2}{\delta^3} \left[ 1 - \frac{\{\cdot\delta\cdot\}}{\{\cdot r_p \cdot\}} \right], \quad (3.7)$$

$$\omega_p = \sqrt{\frac{z^2 e^2}{\delta^3 \cdot m_p} \left[ 1 - \frac{\{\cdot\delta\cdot\}}{\{\cdot r_p \cdot\}} \right]}. \quad (3.8)$$

It should be noted that, in order to calculate the dipole interaction between the macroparticle and the FMP accurately, formulas (3.7) and (3.8) must take into account the own macroparticle volume and the “overlapping” between the volumes of macroparticle and its electrostatic image near the coordinate origin. In the software package RFEHPF.m, this situation is corrected at shifts  $\delta < 2r_p$ ; namely, the dipole contribution is determined exactly by integrating over the non-overlapping volume parts of the particle and its image, i.e. the electrostatic interaction force between the macroparticle and the FMP is approximated by the integral

$$\vec{f}_{12} = \oint_{(\mathbf{r}_1, \mathbf{r}_2 \notin V_1 \cap V_2)} \frac{\rho_1 \rho_2 (\mathbf{r}_1 - \mathbf{r}_2)}{|\mathbf{r}_1 - \mathbf{r}_2|^3} dV_1 dV_2. \quad (3.9)$$

Formulas (3.1)–(3.9) comprise a complete set of relations required for the parameters of braking radiation emitted in the radio-frequency range by the “particle” subsystem in HPF to be determined in the dipole approximation. Similar formulas for quasi-harmonic oscillations of the electron component are characterized by the different initial electron shift,  $\delta_0 \in (r_p, r_C)$ . The final formulas for the quasi-elastic coefficient  $\mu_e$  of cell  $C_\xi^z$  and the frequency, which depends on the instant acceleration of an electron, look like

$$\mu_e = \frac{\alpha e}{\kappa \delta^2} \left[ \frac{\{\cdot\delta\cdot\}}{|\delta - \delta_0|} - \frac{\kappa e \delta^2 \text{Sign}(\delta - \delta_0)}{\alpha |\delta - \delta_0|^3} \right]; \quad (3.10)$$

$$\omega_e = \sqrt{\frac{\alpha e}{\kappa \delta^2} \left[ \frac{\{\cdot\delta\cdot\}}{|\delta - \delta_0|} - \frac{\kappa e \delta^2 \text{Sign}(\delta - \delta_0)}{\alpha |\delta - \delta_0|^3} \right]}. \quad (3.11)$$

#### 4. Amplitude-Frequency Function of Braking Radiation Emitted by HPF

The intensity of a radio signal emitted by HPF in a certain direction  $\mathbf{s}$  (see Fig. 3) is determined by

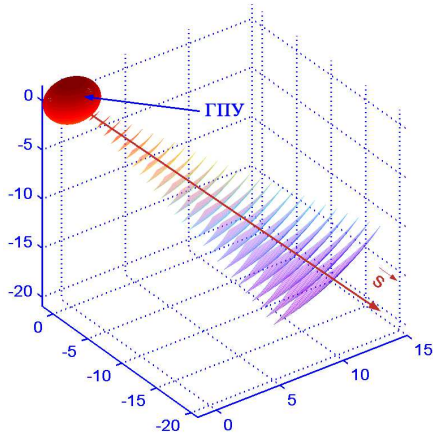


Fig. 3

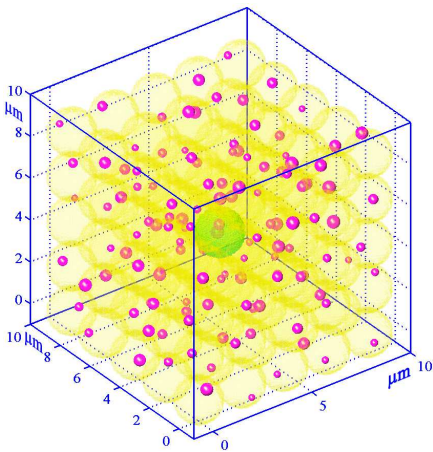


Fig. 4. Element of HPF volume with CDP macroparticles in electroneutral cells

the integrated sum of chaotic radio-wave components emitted by accelerated charges in the plasma formation in all directions. Bearing in mind the stochastic character of braking radiation generated by plasma and leaving aside the issue of electromagnetic radiation (EMR) absorption in a plasma medium, let us determine the qualitative form of the amplitude-frequency function (AFF) for HPF proceeding from the following considerations: (i) the partial contributions to the radio-frequency radiation by accelerated charges in HPF cells are chaotic by both the phase and the frequency, so that the random phase approximation is applicable; in other words, the integrated contribution to the total EMR power is determined in the additive manner; (ii) the averaged intensity of

the braking radiation emitted by HPF cells is spatially isotropic and proportional to the total number of charges accelerated by the self-consistent field in every plasma component; (iii) the relative value of the energy contribution made by a separate cell to the spectral components of HPF braking radiation depends on the statistical probability for a cell to dwell in a definite perturbed state corresponding to a definite shift of the macroparticle or the electron within the cell region. Hence, the density of braking radiation power emitted by HPF in a certain direction  $\mathbf{s}$  can be determined for every spectral component as statistically averaged integrated contributions from all plasma cells. For the frequency  $\omega$  corresponding to the accelerated motion of a separate charge  $z$ , the instant power of radiation emitted into all directions looks like

$$N_{\mathbf{s}} = \frac{2z^2 e^2 |\delta - \delta_0|^2 \omega^2}{3c^3} \sin^2(\omega t). \quad (4.1)$$

Since the process of charge oscillations in HPF is anharmonic, the time averaging for individual charged particles is carried out within the time interval  $[0, \tau]$ , where  $\tau$  is the average relaxation time of a perturbed cell at a given shift of the charge  $z$ , making allowance for variations of the amplitude and the frequency of anharmonic oscillations in the course of relaxation. The energy luminosity of HPF in the radio-frequency range owing to the braking EMR of macroparticles and electrons is a complicated function of the HPF parameters and can be determined on the basis of the derived formulas only in a computer-assisted numerical experiment. As an example, Figs. 4 to 6 illustrate the sequence of the braking EMR initiation in plasma. Owing to turbulent pressure pulsations in plasma, macroparticles, as well as electrons, in separate cells  $C_{\xi}^z$  undergo forced shifts, perturb the charge distribution in the cells (Fig. 5), and accelerate. The relaxation of cells to LTE states occurs as a quasi-harmonic oscillation process resulting in the braking radiation emitted by accelerated charges in HPF in all directions (Fig. 6).

The energy luminosity of HPF in the radio-frequency range is determined firstly by averaging expression (4.1) for separate charges and frequency intervals over the time; then the integration (for the wave zone) over the HPF volume and all frequencies is carried out. Figures 7 to 9 demonstrate the results obtained in the framework of the proposed statistical

approach for the AFF of braking radiation emitted by electrons and macroparticles in HPF. In calculations, we used the conditions of model experiment [18] dealing with the measurements of oscillations of leakage currents from a plane condenser, in which the role of substrate was played by a torch of products of powdered aluminum combustion in air. As was shown in work [11], the mechanism of current oscillations in a condenser in the course of the cited experiments [18] has the same basis as the braking radiation by macroparticles does, namely, a quasi-harmonic oscillation motion of macroparticles and electrons in the self-consistent field in plasma. In the case with a condenser, oscillations of a macroparticle induce variations of the local dielectric permittivity in the torch of combustion products and, consequently, in the condenser capacity at corresponding frequencies. For the braking radiation, every frequency component of anharmonic oscillation charge motion directly initiates variations, with the same frequency, in the spectral components of a radio signal. Therefore, having measured, in that or another way, the amplitude distribution of oscillation modes for the dielectric permittivity of a condenser with a plasma substrate (e.g., by fixing the leakage currents, as was done in work [18]) and comparing it with the distribution of the braking-radiation spectral intensity in a torch, it is possible, in the framework of the inverse problem, to study the microstructure and the ionization characteristics of combustion product plasma. It should be noted that the AFF mode frequencies determined from the analysis of leakage current oscillations [18] and on the basis of the formulas given in this work can have insignificant discrepancies as a result of neglecting the viscosity of a buffer gas, radiation friction, and ponderomotive forces in the non-uniform field of the cell. Those effects are taken into account in the subroutines of software package RFEHPF.m by appending the corresponding terms to the expressions for the coefficient of cell quasi-elasticity  $\mu$ . Figure 7 demonstrates the results of calculations for the contribution of the braking radiation power from electrons in a unit volume of HPF to its total energy luminosity plotted in the  $(\delta_0, \delta)$  coordinate plane. The calculations were carried out for the experimental conditions of work [18].

The statistical probability for electrons to have a certain shift with respect to the equilibrium position in the cell was taken into account by calculating the

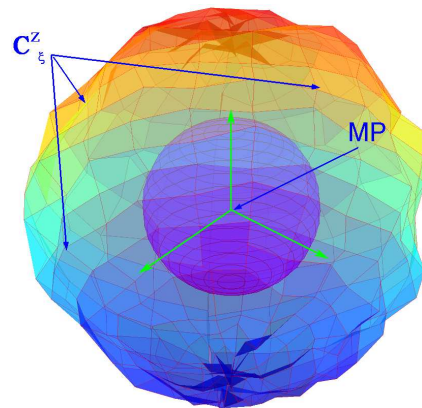


**Fig. 5.** Instant electron-neutral cell in HPF with a macroparticle located at the origin of the reference frame co-moving with the cell

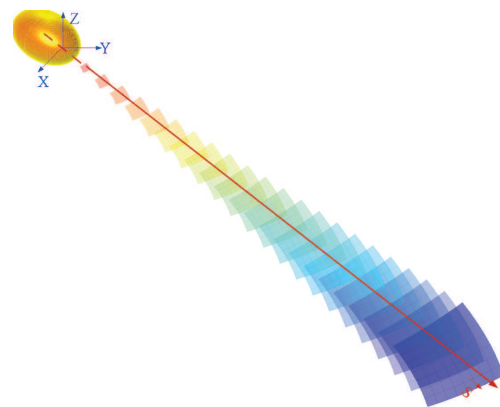


**Fig. 6.** Heterogeneous plasma formation and braking radiation emitted by it in the direction  $s$

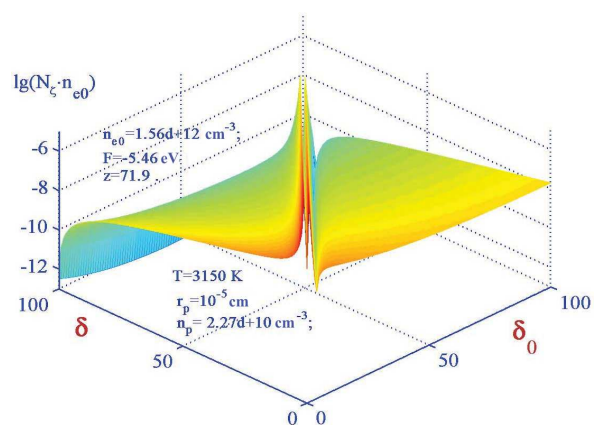


**Fig. 7.** Power of braking radiation emitted by a unit volume of plasma with  $\text{Al}_2\text{O}_3$  (aluminum oxide) nanoparticles

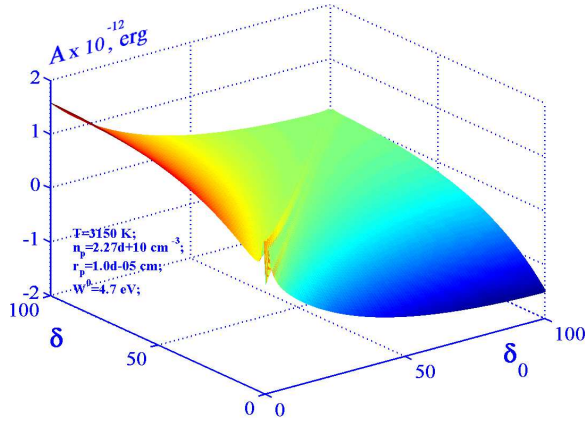


**Fig. 8.** Dependence of the HPF cell energy,  $C_{\xi}^z$ , on the fluctuation-induced shift of a electron with respect to its equilibrium position  $\delta_0$

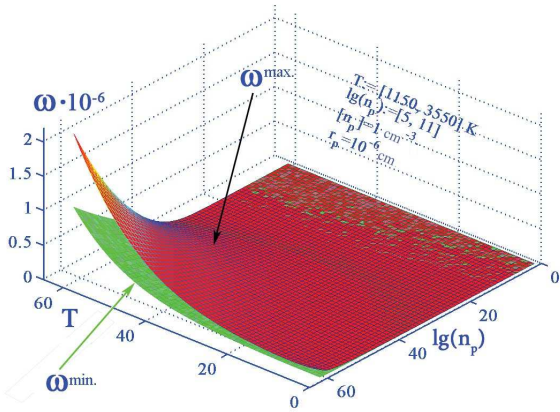


**Fig. 9.** Limits of the frequency range for the braking radiation emitted by aluminum oxide macroparticles in plasma with the CDP

**Table 2. Parameters of high-temperature plasmosol formed by the products of dispersed aluminum combustion in an oxidizing medium**

No.	$T$	$\lg(n_{e0})$	$z$	$F$ , eV	$\lg(\omega^{\min})$	$\lg(\omega^{\max})$
1	3150	10.922	9.5395	-6.256	5.4802	5.8016
2	3190	10.945	10.043	-6.3266	5.5025	5.8306
3	3230	10.966	10.555	-6.3973	5.5241	5.8588
4	3270	10.987	11.078	-6.4682	5.5451	5.8861
5	3310	11.007	11.61	-6.5391	5.5655	5.9127
6	3350	11.027	12.154	-6.6102	5.5854	5.9385
7	3390	11.046	12.708	-6.6814	5.6047	5.9638
8	3430	11.065	13.274	-6.7526	5.6237	5.9884
9	3470	11.084	13.852	-6.8239	5.6422	6.0126
10	3510	11.102	14.443	-6.8951	5.6603	6.0362
11	3550	11.119	15.048	-6.9664	5.6781	6.0595

work executed by the field forces or the external ones and spent to the corresponding deformation (Fig. 7). In the framework of the numerical experiment, the limiting frequencies for the spectral components emitted by macroparticles in the indicated intervals of the key HPF parameters were found. The last two columns of Table 2 hold the indicated frequency values for aluminum oxide macroparticles in the temperature interval  $T = 3150 \div 3550$  K. The calculations were carried out for the initial experimental data of work [17] for a plasmosol of  $\text{Al}_2\text{O}_3$  particles. In heterogeneous plasma with the parameters  $T = 3150$  K, the macroparticle radius  $r_p = 10^{-6}$  cm, and the particle concentration  $n_p = 10^{11}$   $\text{cm}^{-3}$  (the first row in Table 2), the cyclic frequencies of macroparticle oscillations in the combustion product plasma of a model fuel fall within the interval  $\omega \in [\omega^{\min}, \omega^{\max}] = [3.0213 \times 10^5 \text{ s}^{-1}, 6.3329 \times 10^5 \text{ s}^{-1}]$ , which corresponds to the frequency interval  $\nu \in [4.8086 \times 10^4 \text{ Hz}, 1.0079 \times 10^5 \text{ Hz}]$ . According to work [18], the size and the concentration of macroparticles in the combustion product plasma at the temperature  $T = 3150$  K amounted to  $r_p = 9.9256 \times 10^{-6}$  cm and  $n_p = 4.6126 \times 10^9 \text{ cm}^{-3}$ , respectively. The computer-assisted numerical experiment with the help of software subroutine package RFEHPF.m and the indicated set of key plasma parameters resulted in the minimum cyclic frequency of macroparticle oscillations in plasma  $\omega^{\min} = 1.6103 \times 10^5 \text{ s}^{-1}$  and the corresponding frequency  $\nu^{\min} = 2.5629 \times 10^4 \text{ Hz}$ . The experimental value  $\nu^{\min} = 24.5 \text{ kHz}$  coincides with the theoretical one to within a relative error of about 4.6%. Hence, the proposed model of stochastic oscillation motion of charges in the HPF reproduces the experimental situation well. Notice that the processes of macroparticle energy dissipation owing to the viscosity and the radiation friction were not taken into consideration while calculating  $\nu^{\min}$ . Their account reduces the  $\nu^{\min}$ -value, i.e. favors a more exact approximation of experimental data by the model theory describing anharmonic oscillations of macroparticles under the conditions taking place in HPFs.

Figures 10 to 12 demonstrate those cell regions (in the  $(\delta_0, \delta)$ -coordinates) that give partial contributions to the emitted radio power in separate frequency intervals. The integration over the volumes of HPF cells with regard for the statistical probability for every of them to be in a certain perturbed state induced by

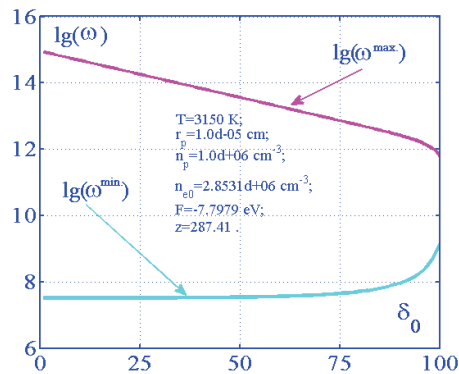


**Fig. 10.** Limits of braking radiation frequencies for electrons arising in the HPF volume owing to their thermal emission from the surface of nanosized macroparticles

the shift of a separate charge gives a contribution to the total power of a plasma radio signal at the given frequency. The intensity of a certain spectral component in the radio signal is provided by emitting electrons that are localized, with a definite probability, in the cell bulk regions confined by the curves in the 2D-plots in Figs. 11 and 12. For instance, in Fig. 11, the bulk regions of cells, where the electrons generating radio-waves at Hz-frequencies are localized, are shifted by the distances reflected by points in the plot plane between the curves marked as “ $10^{12}$ ”. In addition, as follows from the analysis of curves in Fig. 12, only electrons that had initial radial positions and undergo shifting give contributions to radiation at the definite frequency; the corresponding dependences for those contributions cross the limiting straight lines for the given frequencies of braking radiation. At the level of the mechanism describing the emergence and the evolution of quasi-harmonic oscillation electron modes, this circumstance is explained by the fact that the gradient of the total electric field in a perturbed cell falls down in the direction from the macroparticle surface toward the cell periphery. At the same time, for the component “electron–image”, this gradient, on the contrary, grows by the absolute value in the same direction if the relative shift of the image is small.

The results of the presented statistical approach to the description of electrophysical processes in heterogeneous plasma can be taken as a basis while developing methods for the determination of the HPF component content and the volume-averaged electrophysical parameters of the gas and the ensemble of CDP particles on the basis of relative intensities

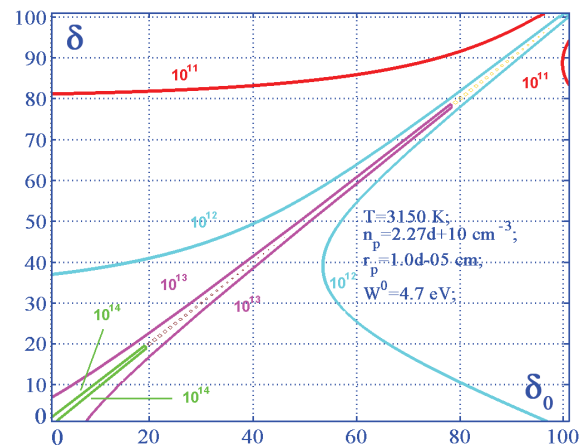


**Fig. 11.** Spatial localization of electrons generating radio waves within the indicated frequency intervals plotted in the  $(\delta_0, \delta)$ -coordinates

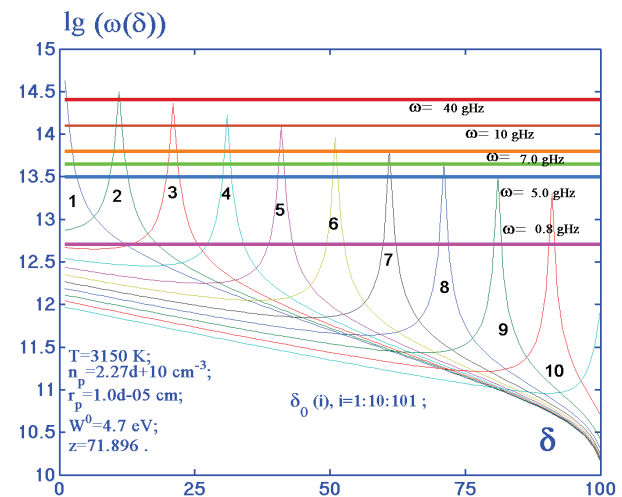


**Fig. 12.** Partial contributions made by interlayers of macroparticle electron atmospheres to the total power of HPF braking radiation

of braking-radiation spectral components within the radio-frequency range. In particular, in the case of the combustion products of solid rocket fuels, there is a capability to determine the temperature and the kind of CDP macroparticles by analyzing the AFF for the radio signal of braking radiation and solving the inverse problem. Together with the more accurate determination of the electron characteristics for nanostructured objects [19, 20], the results of the proposed statistical approach can be applied to the consideration of the properties of HPFs with a polydispersed

condensed phase, which is formed as a result of the agglomeration of nanosized macroparticles.

## 5. Conclusions

1. For the first time, by applying the statistical “cell” approach to the description of electron-ion processes in heterogeneous plasma formations (HPFs), an adequate model is proposed for the emergence of anharmonic oscillation motion by separate macroparticles and electrons in HPFs in a self-consistent field of long-range Coulomb forces, and the corresponding mechanism of evolution is studied.

2. The many-particle problem for the determination of oscillation modes of charged macroparticles in HPF – in particular, the combustion products of solid rocket fuels – was reduced to an effective one-particle one, namely, the research of oscillation motion of a selected macroparticle in the self-consistent perturbed field of electroneutral statistical cell. By separating the stochastic and regular components of the charge motion, an equation for the “restoring” force acting on a charged particle shifted from its equilibrium position in the electroneutral statistical cell of HPF is derived. Partial contributions of plasma charges to the spectral components of the braking radio emission at various stages of their anharmonic oscillation motion are determined.

3. A general statistical concept of HPF braking radiation is proposed. It is based on the separation of the motion of separate plasma particles (macroparticles and electrons) in the effective field of an electroneutral cell into the regular and stochastic components. Radiation emission of electromagnetic waves by accelerated charges shifted from their equilibrium positions is presented as the evolution of the instant stages of their anharmonic oscillations in the course of perturbed cell relaxation of the equilibrium state.

4. The distributions of effective electrophysical parameters in the regions of local thermodynamic equilibrium and their dependences on the key HPF parameters, as well as the spectrum of oscillation modes of charged particles in the condensed dispersed phase, are determined. In the space of thermodynamic parameters, the region of the emergence of plasma instabilities associated with the “particle” component is studied.

5. The amplitude-frequency function (AFF) is determined for the braking radiation of macroparticles

and electrons in the radio-frequency range making allowance for the forces of “effective oscillators” (accelerated charges) in the random phase approximation and with regard for the statistical distribution of electroneutral cells in HPF over the corresponding excitations. In the computer-assisted numerical experiment carried out with the help of the software subroutine package RFEHPF.m, the diagrams describing the dependences of the limiting parameters of oscillation modes on the key HPF parameters are plotted. The studied intervals of HPF parameters are  $T = 1150 \div 3950$  K,  $n_p = 10^5 \div 10^{12}$  cm<sup>-3</sup>,  $r_p = 10^{-7} \div 10^{-4}$  cm,  $W^0 = 4 \div 7$  eV,  $E_F^0 = 5 \div 8$  eV, and  $\varepsilon_p = 5 \div 12$ , which are typical of technological kinds of plasma with a condensed dispersed phase, cover the set of plasma parameters that are actual for applications and single out the region, where oscillation instabilities arise.

6. The frequencies of braking radiation emission and the functional dependences of its intensity on thermodynamic parameters are determined for HPF regions in the locally equilibrium states. Analytical expressions for partial powers of braking-radiation spectral components in thermal plasma with a condensed dispersed phase (CDP) are derived. The AFF of HPF radio emission is shown to possess a characteristic local maximum induced by the most probable perturbations of electroneutral cells in plasma owing to stochastic shifts of the individual charges.

7. The results of experiment [18] dealing with the determination of spectral components for the oscillating sporadic leakage currents from a plane condenser with a plasma torch of products of powdered aluminum combustion in air between the condenser plates and a constant potential difference between the latter are analyzed. A mechanism of emergence of oscillations, which is based on the consideration of fluctuation-induced changes of oscillation modes in the subsystem of CDP particles (aluminum oxide) in the volume of a torch, which plays the role of a plasma-like condenser interlayer, is proposed. For the initial parameters of experiment aimed at studying the oscillation processes in heterogeneous plasma with aluminum oxide particle [18] and in the framework of the proposed model, the electrophysical parameters of plasma and the oscillations spectrum of “particle” component are found. A good theoretical reconstruction with the use of no fitting parameters is obtained for the AFF parameters that are found

for HPFs experimentally. Possibilities of applying the proposed approach to the problems of telediagnosics of heterogeneous plasma formations are discussed in brief.

1. R.A. Treumann and W. Baumjohann, *Advanced Space Plasma Physics* (Imperial College Press, London, 2001).
2. A.G. Zagorodny, I.V. Rogal, A.I. Momot, and I.V. Schweigert, *Ukr. J. Phys.* **55**, 29 (2010).
3. V.N. Tsytovich, G.E. Morfill, S.V. Vladimirov, and H.M. Thomas, *Elementary Physics of Complex Plasmas* (Springer, Berlin, 2008).
4. V.V. Yaroshenko, S.V. Vladimirov, and G.E. Morfill, *New J. Phys.* **8**, 201 (2006).
5. N. Otani and A. Bhattacharjee, *Phys. Rev. Lett.* **78**, 1468 (1997).
6. V.I. Marenkov, *Physical Models of Plasma with Condensed Disperse Phase* (UMK VO, Kiev, 1989) (in Russian).
7. V.I. Marenkov and A.Yu. Kuchersky, *Phys. Aerodisp. Syst.* **45**, 116 (2008).
8. V.I. Marenkov, in *Proceed. of the 24-th Symposium on Plasma Physics and Technology* (EPS, Prague, Czech Republic, 2010), p. 130.
9. V.I. Marenkov, in *Proceed. of the 24-th Conference on Disperse Systems* (Odessa Univ., Odessa, 2010), p. 210 (in Russian).
10. V.I. Marenkov, *J. Mol. Liq.* **120**, 181 (2005).
11. V.I. Marenkov, *Odessa State Univ. Her.* **8/2**, 256 (2003).
12. T. Tesfamichael *et al.*, *Appl. Surf. Sci.* **253**, 4853 (2007).
13. H.L. Pécseli, *Waves and Oscillations in Plasmas* (CRC Press, Univ. of Oslo, Oslo, 2012).
14. R.A. Treumann and W. Baumjohann, *Advanced Space Plasma Physics* (Imperial College Press, London, 2001).
15. I.H. Hutchinson, *Principles of Plasma Diagnostics* (Cambridge Univ. Press, Cambridge, 2005).
16. P.K. Shukla and A. Mamun, *Introduction to Dusty Plasma Physics* (Institute of Physics, Bristol, 2002).
17. V.E. Fortov, A.G. Khrapak, S.A. Khrapak, V.I. Molotkov, and O.F. Petrov, *Phys. Usp.* **47**, 5 (2004).
18. N.I. Poletaev, A.V. Florko, Yu.A. Doroshenko, and D.D. Polishchuk, *Ukr. J. Phys.* **53**, 1066 (2008).
19. V.I. Marenkov, in *Nanomaterials: Applications and Properties*, edited by A. Pogrebnjak, T. Lyuty, S. Protsenko (Sumy Univ., Sumy, 2011), Vol. 2, p. 82.
20. V.I. Marenkov, in *Proceedings of the 14-th International Conference on the Physics and Technology of Thin Films and Nanosystems* (PreCarpathian National Univ., Ivano-Frankivsk, 2013), p. 317.

Received 28.09.04.

Translated from Ukrainian by O.I. Voitenko

*В.І. Маренков*

#### РАДІОВИПРОМІНЮВАННЯ НАНОЧАСТИНОК ГЕТЕРОГЕННІ ПЛАЗМИ З КОНДЕНСОВАНОЮ ДИСПЕРСНОЮ ФАЗОЮ

Резюме

На основі статистичного “чарункового” підходу до опису іонізації гетерогенної плазми (ГП) вивчено механізм генерації гальмівного радіовипромінювання в об’ємі гетерогенних плазмових утворень. Запропоновано нову модель опису ефективної взаємодії мікрополів і зарядів у плазмі. Стохастичний рух заряджених частинок ГП розглядається в моделі як еволюціонуючий процес ангармонічних коливань окремих зарядів у миттєвому полі електричних сил чарунки електронейтральності. Ефективні значення частот і питома інтегральна потужність гальмівного випромінювання ГП в радіодіапазоні визначаються як середні за ансамблем чарунк. Амплітудно-частотна функція і відносні внески окремих коливних мод зарядів плазми в інтенсивність радіовипромінювання знайдені в наближенні хаотичних фаз. У просторі визначальних параметрів ГП проведено порівняльний аналіз даних модельної теорії та експерименту для плазми з наночастинками оксиду алюмінію. Відзначено добре як якісне, так і кількісне узгодження результатів комп’ютерного – в рамках моделі, і натурного експериментів. Обговорено можливості застосування отриманих результатів для завдань теледіагностики гетерогенних плазмових утворень.